THE BALTIC JOURNAL
OF ROAD AND BRIDGE ENGINEERING

ISSN 1822-427X print / ISSN 1822-4288 online
2014 Volume 9(2): 115–122

COMPOSITE DECK IN TWO-DIMENSIONAL MODELLING OF RAILWAY TRUSS BRIDGE

Wojciech Siekierski

Dept of Bridges, Poznań University of Technology, ul. Piotrowo 5, 61-138 Poznań, Poland
E-mail: Wojciech.Siekierski@put.poznan.pl

Abstract. The paper shows a technique of two-dimensional modelling of railway truss bridge girders. The model accounts for joint action of girders and steel-concrete composite deck. Namely, influence of the deck on span flexural rigidity and internal force distribution in truss members are taken into account. The technique is capable of reflecting various arrangements of cross beam to truss flange connection as well as various concrete slab longitudinal rigidity (uncracked/cracked). Application example of test loaded bridge span is given. The accuracy of assessment of span flexural stiffness and internal forces distribution of presented procedure is similar to 3*D* beam/shell element model results accuracy. The presented technique is suitable for preliminary design of truss bridges and verification of other computational methods.

Keywords: railway truss bridge, truss girder, composite deck, joint action, test loading, two-dimensional modelling, numerical verification.

1. Construction and assessment of truss bridges with composite deck

Contemporary railway decks support gravel bed and railway track. This type of track makes the structure less sensitive to vibrations (due to greater inertia) and enables mechanical track maintenance. The deck is made of steel (Ahlgrimm, Lohrer 2005; Dorrer 2009) or concrete (Kim, Shim 2009). Concrete slab is usually connected to steel cross beams – "composite deck" (Hou, Ye 2011; Pedro, Reis 2010; Siekierski 2010). Steel studs are usually used as shear connectors (Shim *et al.* 2014; Xu, Sugiura 2013, 2014; Xu *et al.* 2012, 2014; Xue *et al.* 2012). Figs 1 and 2 show an example of truss bridge with composite deck. Cross beams of the deck transfer loads to truss girders that. They are usually Warren–type trusses (Ahlgrimm, Lohrer 2005; Cheng *et al.* 2013a, 2013b; Dorrer 2009; Kalanta *et al.* 2012). In the case of long spans the spacing of truss flange nodes adjacent to deck is greater than cross beam spacing. Thus truss flange of significant flexural rigidity is required to carry bending caused by mid–node cross beams (plate

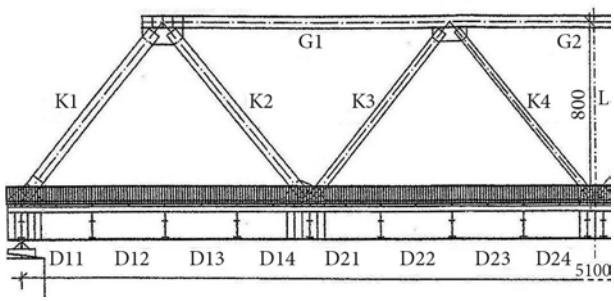

Fig. 1. General view of truss bridge with composite deck

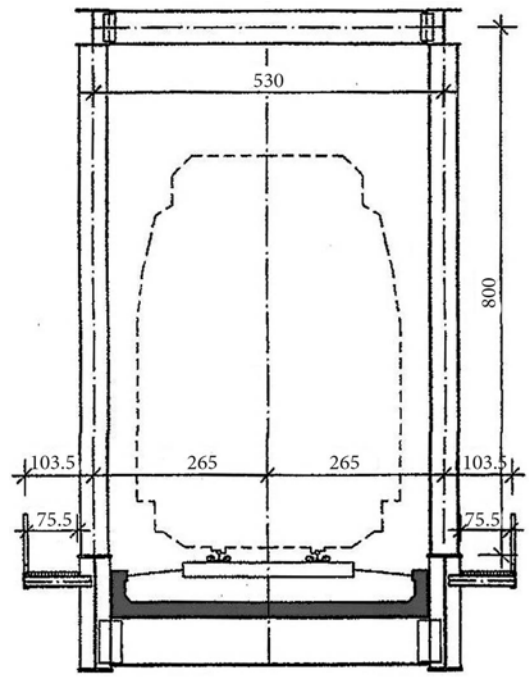

Fig. 2. Cross-section of railway bridge span with composite deck (concrete slab shaded)

doi:10.3846/bjrbe.2014.15

or box girders are used). Such arrangement is present not only in truss bridge spans but in truss-stayed bridges (Reintjes, Gebert 2006) and in trussed decks of modern cable-stayed bridges (Zongyu 2012) as well.

Fig. 3 gives an example of connection of composite deck (namely cross beam) to truss flange connection. The cross beam web is connected to flange web stiffener. This connection is stiffened in horizontal plane by wind bracing gusset plate. The gusset plate extends up to the connector (between concrete slab and cross beam) nearest to the truss flange (Fig. 3). The part of cross beam between truss flange web and the connector is actually a steel beam.

The response of the span under loading depends mainly on truss girders. However, joint action of girders and composite deck is possible. To assume so, the following conditions concerning deck members must be met:

a) cross beams are able to transfer part of longitudinal forces from truss flanges to concrete slab;

b) connectors between cross beams and concrete slab are able to transfer shear forces orthogonal to transverse beams (along span);

c) the slab is able to carry longitudinal forces transferred from connectors; if the slab is in tension and cracked, sufficient reinforcement must be provided.

To verify the conditions mentioned above it is necessary to complete the assessment of railway truss bridge with composite deck in the following stages:

– stage I: setting computational model based on assumptions concerning deck contribution to overall load carrying capacity of the span;

– stage II: checking obtained internal forces in the deck members against their assumed load carrying capacity;

– stage III: if the requirements are not satisfied, it is necessary to repeat the stage I under the assumptions of lack of truss girders and deck cooperation.

Fig. 3. Example of cross beam to truss girder flange connection; wind bracings gusset plate is visible; picture taken prior to casting of concrete slab

2. Two-dimensional modelling and railway truss bridges with composite deck

Progress in structural modelling makes computational models of bridges more and more complex. However, one must remember that complex modelling requires more accurate data. This applies to structural geometry, structural materials and loading. The requirements are not the only reasons for constant popularity of simpler methods of structural modelling. Two-dimensional (2*D*) beam-element modelling is the most common of them.

2*D* analysis is chosen due to its effectiveness. Accuracy of results is often sufficient for engineering purposes (Brencich, Gambarotta 2009). Sophisticated computational model analysis is often accompanied by 2*D* analysis for verification purposes (Liao, Okazaki 2009). Some analytical methods that are still applied in bridge design are based on 2*D* modelling of structures (Machelski 1998).

Truss bridges consist of 1*D* elements (one dimension is relatively much bigger than the other two) and 2*D* elements (one dimension is relatively smaller than the other two). For such structures usually three-dimensional (3*D*) computational models are created (Brencich, Gambarotta 2009; Caglayan *et al.* 2012).

However, in the case of the single-track railway truss bridges the deck length/width ratio is quite substantial even for spans of modest lengths. Thus, for this kind of structures the 2*D* modelling is also justified, especially in terms of determination of vertical loading effects on truss girders at preliminary design stage or as a verification of results provided by more complex model analysis.

One of the problems that arise in 2*D* modelling of bridge spans accounts for joint action of bridge girders and bridge deck. In the case of composite deck, the deck slab may be considered as flexibly connected to the truss girders. Determination of the flexibility may be crucial for setting proper 2*D* model of truss bridge span.

With this purpose, prior to setting computational model, the structural detailing of deck components has to be examined. It is necessary to determine the following:

a) type of cross beam to truss flange connection;

b) material, type and arrangement of connectors;

c) material, dimension and reinforcement of concrete slab.

The data are necessary to find rigidity of cross beams to truss flange connection and longitudinal rigidity of the deck itself.

The following cases are possible:

a) in terms of cross beams to truss flange connection:

case a1) "strong" connection in horizontal plane – cross beam web and flanges are connected or only cross beam web is connected and there is a stiffener (i.e. wind bracings gusset plate) in horizontal plane,

case a2) "weak" connection in horizontal plane – only cross beam web is connected and there is no stiffener in horizontal plane,

b) in terms of longitudinal rigidity of the deck, there are two factors: shear connectors and reinforced concrete slab. The following cases are possible:

case b1) connector system is able to carry shear forces, lateral to cross beams, and concrete slab is able to carry tensile forces as uncracked,

case b2) connector system is able to carry shear forces, lateral to cross beams, and concrete slab is able to carry tensile forces as cracked, but with sufficient reinforcement.

Flexural rigidity of cross beams in horizontal plane between the edge of deck slab and truss flange may be determined on the basis of observation of structural detailing. Longitudinal rigidity of the deck slab itself depends on analysis results. Concrete slab may behave as uncracked or cracked depending on magnitude of longitudinal tensile forces. The obtained internal forces have to be checked against appropriate load carrying capacities to identify the right case.

All that structural features may be reflected in 2*D* model of truss bridge with composite deck.

3. Equivalent characteristics of truss flange adjacent to composite deck in 2*D* computational model

If the assumption is made that the composite deck is capable of joint action together with main girders, then the 2*D* model setting requires assessment of the influence of composite deck on span stiffness and internal forces distribution. Common approach is to introduce equivalent characteristics of the truss flange adjacent to the deck.

This approach, due to its effectiveness, is used in practice (Karlikowski 1995). There an additional analysis is carried out. Computational model is shown in Fig. 4. The model consists of bridge deck and truss flanges (marked with symbols D1–D6) adjacent to it. The analysis of flanges elongation under tensile forces is put versus elongation of flanges themselves (without the deck). Thus, equivalent cross-section of flanges with regard to deck influence on longitudinal stiffness may be computed. Field test proved that this approach improved assessment of actual span flexural stiffness in comparison to 2*D* model based on the stiffness of truss girders only.

Though effective the procedure is rather time-consuming. Relatively large part of the whole structure had to be modelled to accomplish the aim of the analysis, i.e. setting equivalent cross-section area of bottom flange members.

Here, for composite deck a different technique is suggested. A member of truss flange adjacent to the deck between two subsequent cross beams is analysed – Fig. 5.

The meaning of symbols in the Fig. 5 is as follows: N – total force applied to the system, kN; P_a – force transferred by bottom flange member, kN; P_c – force transferred by concrete slab, kN; d – distance between truss flange longitudinal axis and the first connector between cross beam and concrete slab, m; r – cross beam spacing, m; E_a – elastic modulus of steel, kPa; E_c – elastic modulus of concrete, kPa; A_a – cross section area of bottom flange member, m^2; A_c – half of cross-sectional area of the concrete slab, m^2; I_{ah} – moment of inertia of steel part of cross beam in horizontal plane, m^4.

For the system shown in Fig. 5 it is assumed that:

– neutral axes of truss flange member, concrete slab and cross beam are in the same plane,

– truss flange member and concrete slab are rigid enough not to bend in horizontal plane.

Then the steel part of cross beam, of length d, may be assumed as rotationally fixed at both ends.

Thus, a steel part of cross beam acts as the element in Fig. 6. The relationship between R and w, in Fig. 6, is:

$$R = \frac{12E_a I_{ah}}{d^3} w, \tag{1}$$

where E_a – elastic modulus of steel, kPa; I_{ah} – moment of inertia of steel part of cross beam in horizontal plane, m^4; d – distance between rotationally fixed cross-sections in Fig. 6, m; w – relative displacement of the two sections in the direction of force R (orthogonally to the member), m.

For the system shown in Fig. 5 similar equation may be written:

$$N - P_a = \frac{12E_a I_{ah}}{d^3}\left(\Delta l_a - \Delta l_c\right), \tag{2}$$

where Δl_a – elongation of truss flange member, m; Δl_c – elongation of concrete slab, m.

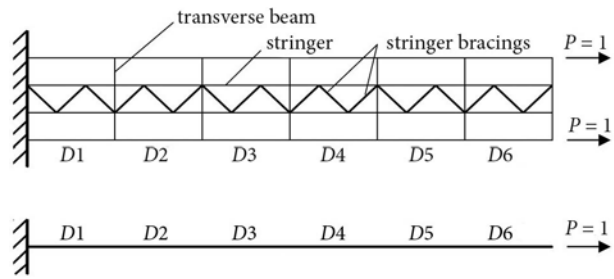

Fig. 4. Additional analysis to set equivalent cross-sections of truss flange members

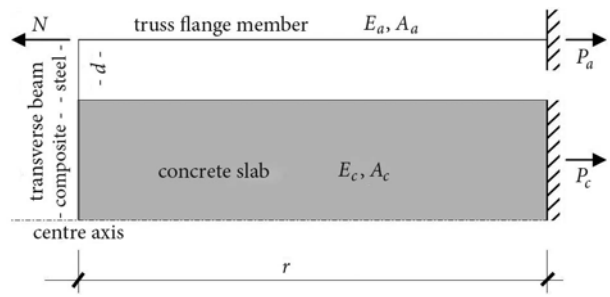

Fig. 5. General scheme of analysis of the truss flange member adjacent to deck

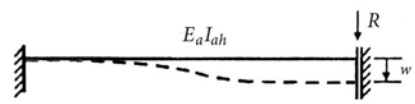

Fig. 6. Beam rotationally fixed at both ends under concentrated load at one of its ends

Equilibrium of forces requires:

$$N - P_a = P_c, \tag{3}$$

Elongation of truss flange member and half of the deck slab, respectively, are:

$$\Delta l_a = \frac{P_a r}{E_a A_a}, \tag{4}$$

$$\Delta l_c = \frac{P_c r}{E_c A_c}. \tag{5}$$

Substituting Eqs (3)–(5) for P_c, Δl_a and Δl_c in Eq (2) gives:

$$N - P_a = \frac{12 E_a I_{ah}}{d^3}\left(\frac{P_a r}{E_a A_a} - \frac{(N - P_a) r}{E_c A_c}\right), \tag{6}$$

hence

$$P_a = \frac{\left(d^3 \beta A_c + 12 I_{ah} r\right) A_a N}{d^3 A_a \beta A_c + 12 I_{ah} r\left(\beta A_c + A_a\right)}, \tag{7}$$

where $\beta = \frac{E_c}{E_a}$. In the equation: E_c – elastic modulus of concrete, kPa; E_a – elastic modulus of steel, kPa.

Equivalent cross-sectional area of truss flange must provide equality of its elongations and the elongation of the truss flange as part of the complex system shown in Fig. 4 that is:

$$\frac{Nr}{E_a A_{a\,equ}} = \frac{P_a r}{E_a A_a}, \tag{8}$$

therefore

$$A_{a\,equ} = \frac{N}{P_a} A_a. \tag{9}$$

Substituting Eq (7) for P_a in Eq (9) gives:

$$A_{a\,equ} = \frac{d^3 A_a \beta A_c + 12 I_{ah} r\left(\beta A_c + A_a\right)}{d^3 \beta A_c + 12 I_{ah} r}. \tag{10}$$

Equivalent cross-sectional area of truss flange member, A_{equ}, takes into account contribution of the composite deck to longitudinal stiffness of that truss flange member in 2*D* computational model.

Eq (10) is valid if there is no cracking of concrete slab. However, the concrete slab may crack due to combined flexure between and over supports together with elongation due to cooperation with truss girders. In such case it is necessary to make the following modifications in the Eq (10):

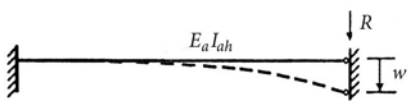

Fig. 7. Clamped/pinned beam under concentrated load at pinned end

a) A_c is to be replaced by cross-sectional area of half of longitudinal reinforcement of the slab;

b) β is to be taken as unity.

If truss flange deforms under cross beam bending in horizontal plane or if cross beam to truss girder flange connection lacks stiffening in horizontal plane, steel cross beam model as in Fig. 6 cannot be assumed. Instead partial rotational restraint of cross beam at its tip near to truss flange member is to be considered.

The degree of the rotational restraint is very hard to establish. It would require laboratory testing of cross beam to truss girder connection for given bridge span with composite deck. Thus the simplified approach is suggested. Equivalent cross-sectional area of truss member is computed as mean of two values:

– equivalent cross-sectional area obtained for model assuming full rotational restraint at both ends of steel part of cross beam;

– equivalent cross-sectional area obtained for model assuming full rotational restraint at the end of steel part of cross beam at first connector and pinned connection of cross beam to truss flange.

The former was discussed above (Fig. 6). The latter is given in Fig. 7. Equivalent area of flange member cross-section is computed from Eq (11):

$$R = \frac{3 E_a I_{ah}}{d^3} w, \tag{11}$$

where: d – is the beam length, m; w – is displacement of its pinned end (Fig. 7) under the force R applied there, m.

Thus, the equivalent cross-sectional area of truss girder member is taken as:

$$A_{a\,equ}^{mean} = \frac{A_{a\,equ}^{fixed} + A_{a\,equ}^{pinned}}{2}, \tag{12}$$

where $A_{a\,equ}^{fixed}$ and $A_{a\,equ}^{pinned}$ – equivalent cross-sectional area of truss member flange taken from model in Fig. 6 and Fig. 7 respectively; $A_{a\,equ}^{mean}$ – the mean value of those two.

For all cases described the general provision is made that cross beam to truss flange connection as well as connectors between concrete slab and cross beam are able to transfer forces from truss flanges to the slab.

Thus, the equivalent area of truss flange adjacent to the composite deck regarding the deck and truss girders cooperation in 2*D* model is set.

4. Application example

4.1. Experiment

The test loading of "twin" railway truss spans with composite decks, shown in Fig. 1, was carried out. Their decks are connected to bottom flanges of truss girders at their nodes and between them.

Geometrical data of the "twin" spans are:

– theoretical span length – 51.0 m,

– truss girder spacing – 5.30 m,

– truss girder theoretical height – 8.00 m,

– bottom flange node spacing – 12.75 m,

– cross beam spacing – 3.19 m.

Geometrical characteristics of bridge span member are put together in Table 1. For member symbols see Fig. 1. The explanation of indices: 1) half of element near D11, 2) half of element near D13, 3) half of element near D13, 4) half of element near D21, 5) half of section near D14, 6) half of element near D22.

Fig. 8 shows deck slab cross-section: at mid-span (between cross beams – A–A) and over cross beam web (B–B). Connectors and reinforcing bars is shown. Composite deck construction details are:

– slab transverse expansion joint at mid-span,

– slab thickness: variable, 0.25–0.33 m,

– concrete: f_{cd} ~ 20 MPa, E_c ~ 35 GPa

– longitudinal reinforcement: top and bottom layers of 32 bars of 25 mm diameter of 18G2-b grade steel,

– connectors of angles 160×160×15 mm, with stiffeners.

The same locomotive set was used for both spans (Fig. 9). In the case of both spans the railway track is located symmetrically between truss girders. Thus, four truss girders were test loaded in the same way.

During testing the following were recorded:

– vertical displacement of bottom flange nodes: "$\frac{1}{4}L_t$", "$\frac{1}{2}L_t$", "$\frac{3}{4}L_t$" under loading scheme as in Fig. 9,

– strains at the top of truss bottom flanges at cross-section located 3.5 m away from the "" node towards mid-span, recorded while locomotive set went through the span at very low speed (≤ 5 km/h) – quasi-static loading.

4.2. Numerical verification

To verify the test loading results two computational models were created:

– the 3*D* model consisted of beam elements (truss girders, cross beams, wind bracings), creating space frame, and shell elements (deck slab);

– the 2*D* model consisted of beam elements only.

The 3*D* model (Fig. 10) required shell elements to be placed at the true level of deck slab mid-plane. Hence, kinematic constraints were applied to appropriate pairs of nodes, of cross beams and truss bottom flange to ensure compatibility of displacements. The constraints are shown in Fig. 10 as short vertical elements connecting girders and deck.

The 3*D* model regards eccentricities in truss cross-bracings to bottom flange connections as well as different levels of neutral axes of steel cross beams, composite cross beams, slab mid-plane and supports.

This model was used to assess internal forces acting at cross beam to truss flange connection, shear forces at cross beam to concrete slab connection and longitudinal forces in concrete slab. Preliminary assessment proved that composite deck is able to resist additional internal forces resulted from deck and girders cooperation. Assumption of uncracked concrete slab behaviour was justified.

The 2*D* model was then created. It is shown in Fig. 11. It accounts for composite deck by means of equivalent cross-sectional areas of members of truss flange adjacent to the deck (bottom flange).

Table 1. Cross-sectional characteristics of bridge members

Model element	A_X, cm^2	I_X, cm^4	I_Y, cm^4	I_Z, cm^4
D11, D12[1)]	364	231	1 669 197	33 358
D12[2)], D13, D14[3)]	394	337	1 878 496	39 608
D14[4)], D21[5)]	494	1012	2 586 517	60 441
D21[6)], D22÷D24	474	794	2 466 298	56 274
G1	310	432	158 183	41 711
G2	405	958	221 373	58 398
K1	244	243	37 514	87 208
K2	184	110	25 014	59 471
K3	134	58	12 803	40 572
K4	98	32	4503	27 393
Steel cross beam	170	150	157 119	5 439
Composite cross beam	599	57 000	614 000	810 000

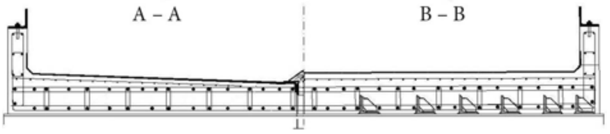

Fig. 8. Cross-section of deck slab: in-between cross beams (A–A) and over cross beam (B–B)

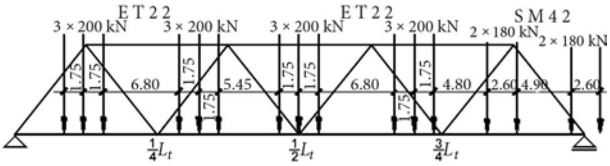

Fig. 9. Analysed test loading scheme with locomotive set

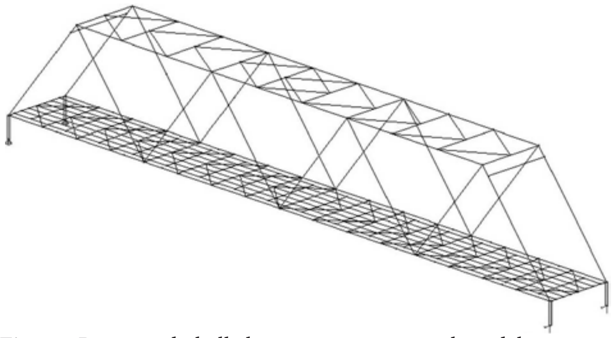

Fig. 10. Beam-and-shell element computational model

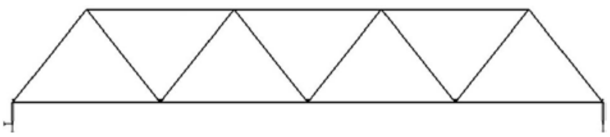

Fig. 11. Beam element computational model

To compute equivalent cross-sectional area of member of truss flange adjacent to deck, the procedure described earlier was applied. Due to limited truss flange flexural rigidity in horizontal plane, partial rotational restraint of cross beam at its connection to truss flange was assumed. Equivalent cross-sectional area of truss flange members was computed according to Eq (10).

The model regards eccentricities in cross-bracings to bottom flange connections, different levels of neutral axes of truss bottom flange members and level of supports as well as the fact that live load is applied to girders at connections of cross beams.

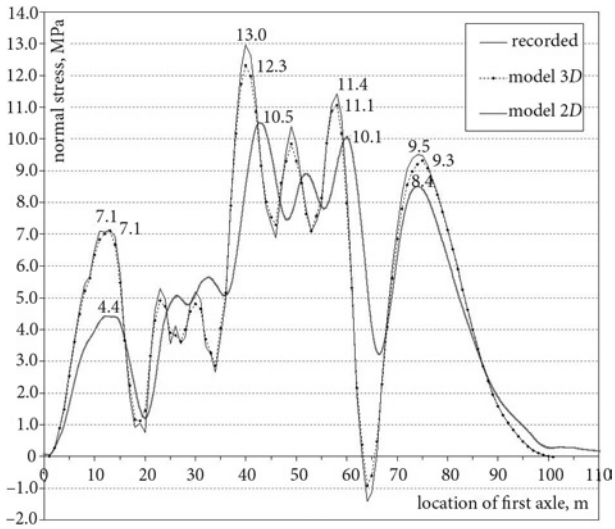

Fig. 12. Strain variations at top fibre of truss bottom flange

Table 2. Equivalent of cross-sectional area of bottom flange members in 2*D* computational model

Model element	A_X, cm^2	Equivalent area		
		A_X^f, cm^4	A_X^p, cm^4	A_X^m, cm^4
D11, D12[1)]	364	684	464	574
D12[2)], D13, D14[3)]	394	714	494	604
D14[4)], D21[5)]	494	814	594	704
D21[6)], D22÷D24	474	794	574	684

Note: indices are the same as for Table 1.

Table 3. Displacement *u*, mm, of bottom flange nodes

Data source	Location of bottom flange node		
	„$\frac{1}{4}L_t$"	„$\frac{1}{2}L_t$"	„$\frac{3}{4}L_t$"
Recorded	8.16	11.78	8.07
Model 3D	9.43	13.35	9.29
Model 2D	9.29	13.21	9.16
Relationship: $\frac{u_{computed}}{u_{recorded}}$			
Model 3D	1.16	1.13	1.15
Model 2D	1.14	1.12	1.14

Characteristics of structural elements were assumed according to design specifications. They are put together in Table 1 (for symbols – Fig. 2).

For the 2*D* model equivalent cross-sectional areas of bottom flange members were computed. The procedure presented above was applied. Uncracked behaviour of concrete slab was assumed. Results are given in Table 2. Moments of inertia of truss bottom flange members were taken as in Table 1.

Table 2 gives three values of equivalent cross-sectional areas for each member of bottom flange. Indices in Table 2 comply with those in Table 1. Explanation of symbols is as follows:

A_X – actual cross-sectional area of flange member,

A_X^f – equivalent cross-sectional area of flange member; assumed fixed end of cross beam at its connection to truss flange,

A_X^p – equivalent cross-sectional area of flange member; assumed pinned connection of cross beam connection to truss flange,

A_X^m – mean equivalent cross-sectional area of flange member; assumed partial rotational restraint of cross beam at its connection to truss flange; computed as mean of A_X^c and A_X^p.

4.3. Recorded versus computed results

Recorded and computed results are presented against each other below.

Table 3 gives the recorded and computed displacements. Recorded values are mean values for population of four truss girders. A positive sign marks displacement downwards.

3*D* and 2*D* computational models were also used to find normal stress at the top fibre of truss bottom flange at analysed cross-section (3.5 m away from the "$\frac{1}{4}L_t$" node towards mid-span). They were computed as follows:

$$\sigma_{3D} = \frac{N_{3D}}{A_X} + \frac{M_{3D}}{I_Y} z, \tag{12}$$

$$\sigma_{2D} = \frac{\kappa N_{2D}}{A_X} + \frac{M_{2D}}{I_Y} z, \tag{13}$$

where σ_{2D}, σ_{3D} – normal stresses based on 2*D* and 3*D* model analysis respectively, kPa; N_{2D}, M_{2D} and N_{3D}, M_{3D} – internal forces obtained from 2*D* and 3*D* model analysis respectively, kN and kNm; A_X – cross sectional area of truss member, m^2; I_Y – moment of inertia of truss member in respect to horizontal axis, m^4; z – distance from truss flange member neutral axis to its top fibre, m; κ is computed as:

$$\kappa = \frac{A_X}{A_X^m}. \tag{14}$$

Fig. 12 presents variations of normal stress based on strains recorded at the top fibre of truss bottom flange and computed according to Eqs (12) and (13).

Table 4 puts together the recorded and computed values of four peaks of the stress diagram.

2*D* and 3*D* computational models overestimate peak stresses in truss flange in comparison to recorded ones. The overestimation of the largest peak is 17% in the case of 3*D* model and 24% in the case of 2*D* model. The difference is caused by bending in horizontal plane and torsion that are not taken into account in 2*D* modelling. In general the accuracy of stress variation assessment provided by both models is similar.

Table 4. Recorded and computed normal stress peaks, MPa, at the top fibre of bottom flange member

Data source	Chart characteristic points			
	Peak 1	Peak 2	Peak 3	Peak 4
Recorded	4.4	10.5	10.1	8.4
Model 3D	7.1	12.3	11.1	9.3
Model 2D	7.1	13.0	11.4	9.5
Relationship: $\frac{\sigma_{computed}}{\sigma_{recorded}}$				
Model 3D	1.61	1.17	1.10	1.11
Model 2D	1.61	1.24	1.13	1.13

5. Conclusions

1. It is possible to use a relatively easy and compact analytical technique to assess composite deck influence on span flexural stiffness and stress level in structural members.

2. The described analytical procedure regards various structural arrangements of cross beam to truss flange connection as well as various deck slab longitudinal rigidity under tensile forces (uncracked/cracked).

3. Equivalent cross-sectional areas of members of truss flange adjacent to the deck, resulted from the procedure, are easy to introduce in 2*D* computational model of truss bridge span.

4. The accuracy of assessment of span flexural stiffness and internal forces distribution provided by the presented procedure is similar to accuracy available in 3*D* beam/shell element model of truss bridge span.

5. The presented approach to railway truss bridge assessment is suitable for preliminary design and verification of other computational methods.

References

Ahlgrimm, J.; Lohrer, I. 2005. Erneuerung der Eisenbahnüberführung in Fulda-Horas über die Fulda [A New Rail Bridge Crosses the River Fulda in Fulda-Horas], *Stahlbau* 74(2): 114–120. http://dx.doi.org/10.1002/stab.200590002

Brencich, A.; Gambarotta, L. 2009. Assessment Procedure and Rehabilitation of Riveted Railway Girders: the Campasso Bridge, *Engineering Structures* 31(1): 224–239. http://dx.doi.org/10.1016/j.engstruct.2008.07.007

Caglayan, O.; Ozakgul, K.; Tezer, O. 2012. Assessment of Existing Steel Railway Bridges, *Journal of Constructional Steel Research* 69(1): 54–63. http://dx.doi.org/10.1016/j.jcsr.2011.08.001

Cheng, B.; Qian, O.; Sun, H. 2013a. Steel Truss Bridges with Welded Box-Section Members and Bowknot Integral Joints, Part I: Linear and Non-Linear Analysis, *Journal of Constructional Steel Research* 80: 465–474. http://dx.doi.org/10.1016/j.jcsr.2012.08.006

Cheng, B.; Qian, O.; Sun, H. 2013b. Steel Truss Bridges with Welded Box-Section Members and Bowknot Integral Joints, Part II: Minimum Weight Optimization, *Journal of Constructional Steel Research* 80: 475–482. http://dx.doi.org/10.1016/j.jcsr.2012.09.012

Dorrer, G. 2009. Die neue Eisenbahnbrücke über den Donaukanal und den Winterhafen in Wien [The New Railway Bridge Across the Donaukanal and the Winterhafen in Vienna], *Stahlbau* 78(2): 70–77. http://dx.doi.org/10.1002/stab.200910007

Hou, W.-Q.; Ye, M.-X. 2011. Design Methods of Headed Studs for Composite Decks of Through Steel Bridges in High-Speed Railway, *Journal of Central South University of Technology* 18: 946–952. http://dx.doi.org/10.1007/s11771-011-0785-4

Kalanta, S.; Atkočiūnas, J.; Ulitinas, T.; Grigusevičius, A. 2012. Optimization of Bridge Trusses Height and Bars Cross-Sections, *The Baltic Journal of Road and Bridge Engineering* 7(2): 112–119. http://dx.doi.org/10.3846/bjrbe.2012.16

Karlikowski, J. 1995. Projekt wzmocnienia mostu kratowego o małej sztywności [Design of Strengthening of Truss Bridge with Low Stiffness], in *Proc. of the 9th International Conference on Metal Structures*: vol. 3. Kraków, Poland, 1995, 261–273.

Kim, H.-H.; Shim, C. S. 2009. Experimental Investigation of Double Composite Twin-Girder Railway Bridges, *Journal of Constructional Steel Research* 65(6): 1355–1365. http://dx.doi.org/10.1016/j.jcsr.2009.02.004

Liao, M.; Okazaki, T. 2009. *A Computational Study of the I-35 Bridge Collapse*. Research Report No. CTS 09-29. Center for Transportation Studies, University of Minnesota. 95 p.

Machelski, C. 1998. Zastosowanie metody kinematycznej do wyznaczania funkcji wpływu sił wewnętrznych w układach prętowych [Application of Kinematics Method to Setting Influence Functions of Internal Forces in Bar-Element Structures], *Inżynieria i Budownictwo* 7(98): 372–375.

Pedro, J. O.; Reis, A. J. 2010. Nonlinear Analysis of Composite Steel-Concrete Cable-Stayed Bridges, *Engineering Structures* 32(9): 2702–2716. http://dx.doi.org/10.1016/j.engstruct.2010.04.041

Reintjes, K.; Gebert, G. 2006. Das Zügelgurt-Fachwerk der Muldebrücke Wurzen [The Truss–Stayed Structure of the Mulde Bridge Wurzen], *Stahlbau* 75(8): 613–623. http://dx.doi.org/10.1002/stab.200610063

Shim, C.-S.; Kim, D.-W.; Nhat, M. X. 2014. Performance of Stud Clusters on Precast Bridge Decks, *The Baltic Journal of Road and Bridge Engineering* 9(1): 43–51. http://dx.doi.org/10.3846/bjrbe.2014.06

Siekierski, W. 2010. Kolejowe przęsła kratownicowe z pasem sztywnym [Railway Truss Bridges with Rigid Flange], *Inżynieria i Budownictwo* 2: 97–99.

Xu, C.; Sugiura, K. 2014. Analytical Investigation on Failure Development of Group Studs Shear Connector in Push-Out

Specimen under Biaxial Load Action, *Engineering Failure Analysis* 37: 75–85. http://dx.doi.org/10.1016/j.engfailanal.2013.11.010

Xu, X.; Liu, Y.; He, J. 2014. Study on Mechanical Behavior of Rubber-Sleeved Studs for Steel and Concrete Composite Structures, *Construction and Building Materials* 53: 533–546. http://dx.doi.org/10.1016/j.conbuildmat.2013.12.011

Xu, C.; Sugiura, K. 2013. Parametric Push-Out Analysis on Group Studs Shear Connector Under, Effect of Bending-induced Concrete Cracks, *Journal of Constructional Steel Research* 89: 86–97. http://dx.doi.org/10.1016/j.jcsr.2013.06.011

Xu, C.; Sugiura, K.; Wu, C.; Su, Q. 2012. Parametrical Static Analysis on Group Studs with Typical Push-Out Tests, *Journal of Constructional Steel Research* 72: 84–96. http://dx.doi.org/10.1016/j.jcsr.2011.10.029

Xue, D.; Liu, Y.; Yu, Z.; He, J. 2012. Static Behavior of Multi-Stud Shear Connectors for Steel-Concrete Composite Bridge, *Journal of Constructional Steel Research* 74: 1–7. http://dx.doi.org/10.1016/j.jcsr.2011.09.017

Zongyu, G. 2012. Zhengzhou Yellow River Road-Cum-Railway Bridge, China, *Stahlbau* 81(2): 151–155. http://dx.doi.org/10.1002/stab.201201522

Received 29 December 2011; accepted 22 June 2012